Calculations on the Auger spectrum of F_2

Christoph-Maria Liegener
Institut für Theoretische Physik, Technische Universität Berlin, Hardenbergstrasse 4-5/IV, D-1000 Berlin 12, West Germany
(Received 19 January 1983)

The core-valence-valence Auger spectrum of the F_2 molecule has been calculated by the particle-particle Green's-function method. Main emphasis has been laid on the intermediate-energy region. The pronounced gap at 621—626 eV has been explained as a consequence of the partial breakdown of the quasiparticle picture for the inner-valence electrons.

I. INTRODUCTION

The core-valence-valence molecular Auger spectra of first-row compounds[1] can mostly be divided into three parts. The first part, highest in energy, results from transitions to final states with holes in two outer-valence orbitals; the lines are strong and narrow. There then follow, towards lower energy, the regions associated with holes in both one inner- and one outer-valence orbital and those with holes in two inner-valence orbitals, the lines becoming more and more smeared out with decreasing energy.

One of the reasons for this smearing out is that in the corresponding energy regions several transitions to shake-up final states occur with comparable probability. This means that the lines of the quasiparticle picture are split into a number of satellites, and if these have comparable intensity it may even be impossible to identify one of them as dominant. Such a more or less complete breakdown of the quasiparticle picture considerably complicates the interpretation of the corresponding regions in the spectrum.

The Auger spectrum of the F_2 molecule has recently been recorded by Weightman, Thomas, and Jennison[2] (WTJ). These authors were also able to give a successful reproduction by theory for the first and third of the above-mentioned regions of this spectrum while, on the other hand, obtaining only poor agreement for the intermediate region. In this study therefore, we shall confine ourselves mainly to the intermediate part of the spectrum.

The breakdown of the quasiparticle picture for inner-valence electrons is most directly accessible by photoelectron spectroscopy.[3] Thus an important characteristic of the method we shall be using here[4] is that it stresses the connections between photoelectron and Auger spectra. In the case of F_2 the experimental photoelectron spectrum does not reveal any satellite structure for the inner-valence orbitals,[2] although the calculations[5] still predict a partial breakdown of the quasiparticle picture for these orbitals. We shall show how this satellite structure in the theoretical photoelectron spectrum is associated with certain structures in the Auger spectrum which are in fact experimentally visible.

II. METHOD

The present calculations employ the Green's-function method. Since the principles of applying this method to Auger spectra have been described elsewhere,[4] we may confine ourselves to a short description. The kinetic energy of an Auger electron is

$$E_{\mathrm{kin}}=E_{\mathrm{IP},c}-E_{\mathrm{DIP},\nu}\ , \tag{1}$$

where IP_c is the core ionization potential, corresponding to the initial state of the Auger process, and DIP_ν is a double ionization potential, corresponding to the final state. IP_c is obtained from the poles of the one-particle Green's function and DIP_ν from the poles of the particle-particle Green's function.

The connection between the Auger spectrum and the photoelectron spectrum of the valence electrons is established by renormalization of the particle-particle Green's function in terms of one-particle Green's-function data. In matrix notation (over two-orbital indices k,l) one obtains the following Bethe-Salpeter equation for the particle-particle Green's function $\mathcal{G}$:

$$\mathcal{G}^{-1}(\omega)=\mathcal{G}^{(0)-1}(\omega)-\mathcal{K}\ , \tag{2}$$

where $\mathcal{K}$ is the first-order irreducible vertex part (for explicit expressions see Ref. 4) and

$$\mathcal{G}^{(0)}_{klmn}(\omega)=\sum_{\mu,\nu}\gamma_{k\mu,l\nu}P_{k\mu}P_{l\nu}\delta_{km}\delta_{\ln}/(\omega-\omega_{k\mu}-\omega_{l\nu})\ , \tag{3}$$

where $\omega_{k\mu}$ is used to denote the poles of the one-particle Green's function (which is assumed to be approximately diagonal[6]) and $P_{k\mu}$ the corresponding pole strengths (residues of the eigenvalues of the Green's-function matrix). By convention,[6] the second index μ of $\omega_{k\mu}$ numbers the various poles arising from the splitting of the orbital energy ϵ_k by many-body perturbation theory. The sum in Eq. (3) runs only over poles with appreciable $P_{k\mu}$ and it is assumed that only such poles are included to keep, for $k\in\mathrm{occ}$, $\omega_{k\mu}$ always less than 0 and to keep, for $k\notin\mathrm{occ}$, $\omega_{k\mu}$ always greater than 0 (occ is the set of orbitals occupied in the Hartree-Fock ground state). The factor $\gamma_{k\mu,l\nu}$ is then -1 for $k,l\in\mathrm{occ}$, $+1$ for $k,l\notin\mathrm{occ}$, and 0 in other cases.

The particle-particle Green's function $\mathcal{G}(\omega)$ has poles at $-\mathrm{DIP}_\nu$. For each transition such a pole is calculated as a zero of an eigenvalue of $\mathcal{G}^{-1}$ from Eq. (2) and the corresponding pole strength as the inverse derivative of that eigenvalue at the pole.

The transition rates (TR's) are obtained by expanding initial and final states into Hartree-Fock states, approximating the expansion coefficients by the residues of the Green's functions,[4] and evaluating the matrix elements be-

TABLE I. One-particle Green's-function data for F_2 (energies in eV).

Molecular orbital	ϵ_k	$\omega_{k\mu}$	$\omega_{k\mu}$[a]	Experiment[b,c]
$1\sigma_g, 1\sigma_u$[d]	−719.31	−782.18(0.100)		
		−696.43(0.748)		−696.65[b]
$2\sigma_g$	−48.42		−56.19(0.13)	
			−41.30(0.13)	−41.75[b]
			−40.53(0.56)	
$2\sigma_u$	−40.89		−36.17(0.71)	−37.47[b]
			−28.81(0.11)	
$3\sigma_g$	−20.22	−20.95(0.917)	−21.03	−21.1[c]
$1\pi_u$	−22.25	−18.98(0.874)	−18.99	−18.8[c]
$1\pi_g$	−18.39	−15.68(0.907)	−15.86	−15.87[c]

[a]Reference 5.
[b]Reference 2.
[c]Reference 14.
[d]The poles for $1\sigma_g$ and $1\sigma_u$ are almost identical.

tween the Hartree-Fock states in the one-center model.[7,8] The explicit expressions for the TR's to singlet (S) or triplet (T) final states are (in atomic units)

$$W_{\mathrm{TR}}^{(S,T)} = 2\pi d^{(S,T)} \sum_{l,m} \sum_{i,j,i',j'} M_{ij}^{(S,T)}(\varphi_{lm}) M_{i'j'}^{(S,T)}(\varphi_{lm}) \times P_c \operatorname*{Res}_{-E_{\mathrm{DIP},\nu}} (-\mathcal{G}_{iji'j'}^{(S,T)}) \quad (4)$$

with $d^{(S)}=1$ and $d^{(T)}=3$; P_c is the pole strength of the core IP and

$$M_{ij}^{(S,T)}(\varphi) = 2^{-1/2}(V_{ijc\varphi} \pm V_{ij\varphi c}), \quad \text{if } i \neq j$$

$$M_{ij}^{(S)}(\varphi) = V_{ijc\varphi}, \quad \text{if } i = j$$

where $\varphi_{lm} = R_l Y_{lm}$ is a continuum orbital centered at the primary ionization site and in the two-electron integrals $V_{ijc\varphi}$ only the one-center atomic integrals are taken into consideration[7,8] and these are expressed[9] in terms of the radial integrals given by McGuire.[10]

TABLE II. Auger spectrum of F_2, calculated using experimental inner-valence IP's (energies in eV, transition rates in 10^{-3} a.u.).

Symmetry	E_{kin}	TR	Dominating components
$^1\Delta_g$	654.80(−0.805)	0.039	$1\pi_g^2(0.712)$, $1\pi_u^2(0.288)$
$^1\Sigma_g^+$	654.67(−0.804)	0.009	$1\pi_g^2(0.689)$, $1\pi_u^2(0.310)$
$^3\Pi_g$	647.27(−0.829)	0.070	$3\sigma_g^1 1\pi_g^3(0.984)$
$^1\Pi_g$	646.23(−0.827)	0.320	$3\sigma_g^1 1\pi_g^3(0.976)$
$^3\Pi_u$	644.80(−0.795)	0.052	$1\pi_u^3 3\sigma_g^1(0.967)$
$^1\Pi_u$	644.01(−0.792)	0.233	$1\pi_u^3 3\sigma_g^1(0.947)$
$^1\Delta_u$	642.74(−0.794)	0.361	$1\pi_u^3 1\pi_g^3(1.000)$
$^1\Delta_g$	642.17(−0.783)	0.334	$1\pi_u^2(0.681)$, $1\pi_g^2(0.319)$
$^1\Sigma_g^+$	641.42(−0.809)	0.106	$3\sigma_g^0(0.418)$, $1\pi_u^2(0.386)$, $1\pi_g^2(0.192)$
$^1\Sigma_u^+$	641.33(−0.790)	0.089	$1\pi_u^3 1\pi_g^3(0.988)$
$^1\Sigma_g^+$	639.94(−0.820)	0.126	$3\sigma_g^0(0.612)$, $1\pi_u^2(0.240)$, $1\pi_g^2(0.131)$
$^3\Pi_u$	634.73(−0.646)	0.020	$2\sigma_u^1 1\pi_g^3(0.848)$, $2\sigma_g^1 1\pi_u^3(0.102)$
$^1\Pi_g$	633.20(−0.628)	0.021	$2\sigma_u^1 1\pi_u^3(0.517)$, $2\sigma_g^1 1\pi_g^3(0.451)$
$^1\Pi_u$	633.03(−0.643)	0.059	$2\sigma_u^1 1\pi_g^3(0.691)$, $2\sigma_g^1 1\pi_u^3(0.230)$
$^3\Sigma_u^+$	629.50(−0.650)	0.022	$2\sigma_u^1 3\sigma_g^1(0.992)$
$^3\Pi_g$	627.52(−0.624)	0.046	$2\sigma_g^1 1\pi_g^3(0.631)$, $2\sigma_u^1 1\pi_u^3(0.367)$
$^3\Pi_u$	625.94(−0.608)	0.034	$2\sigma_g^1 1\pi_u^3(0.879)$, $2\sigma_u^1 1\pi_g^3(0.121)$
$^1\Sigma_u^+$	624.84(−0.651)	0.142	$2\sigma_u^1 3\sigma_g^1(0.989)$
$^1\Sigma_g^+$	622.37(−0.621)	0.081	$2\sigma_g^1 3\sigma_g^1(0.917)$
$^1\Pi_g$	621.60(−0.625)	0.183	$2\sigma_g^1 1\pi_g^3(0.546)$, $2\sigma_u^1 1\pi_u^3(0.446)$
$^1\Pi_u$	620.70(−0.614)	0.161	$2\sigma_g^1 1\pi_u^3(0.733)$, $2\sigma_u^1 1\pi_g^3(0.264)$
$^1\Sigma_g^+$	612.62(−0.517)	0.061	$2\sigma_u^0(0.774)$, $2\sigma_g^1 3\sigma_g^1(0.121)$
$^1\Sigma_u^+$	604.93(−0.496)	0.108	$2\sigma_g^1 2\sigma_u^1(0.966)$
$^1\Sigma_g^+$	602.57(−0.485)	0.064	$2\sigma_g^0(0.863)$, $2\sigma_u^0(0.112)$

III. RESULTS

The calculations were started with a Hartree-Fock calculation using a $(9s\,5p)/[4s\,2p]$ Gaussian basis set[11] per atom at $R_{\text{F-F}}=1.411\,93$ Å.[12] The subsequent one-particle Green's-function calculations employed the second-order irreducible self-energy part for the core IP's and the first seven electron affinities (the virtual counterparts of the core- and inner-valence orbitals were left unrenormalized). For the outer-valence IP's also the third-order diagrams were calculated (in these diagrams only the outer-valence orbitals and their virtual counterparts were considered in the summations) and the geometric approximation[13] was adopted for the irreducible self-energy part. The resulting poles for the core- and outer-valence IP's are listed in the first column of Table I (pole strengths $P_{k\mu}$ in parentheses); only poles with $P_{k\mu}\geq 0.1$ are given. The inner-valence IP's were taken from Ref. 5 and are included in the second column of Table I (the outer-valence IP's of Ref. 5 are also given for comparison). The experimental values of the negative IP's from Refs. 2 and 14 are collected in the last column of Table I.

We note that the theoretical results of Ref. 5 provide more information on the inner-valence electrons than the experimental results. This is so because the partial breakdown of the quasiparticle picture for the inner-valence electrons is not visible in the photoelectron spectrum[2] as mentioned in the Introduction. In a semiempirical approach one could try to use the experimental energies for these inner-valence IP's while estimating the corresponding pole strengths by comparison with theory as $P_{2\sigma_g}\approx 0.69$ and $P_{2\sigma_u}\approx 0.71$, and then build up via Eqs. (2) and (3) the particle-particle Green's function. Such calculations have been performed. The other $\omega_{k\mu}$ used were those of the first column of Table I and also all $\omega_{k\mu}$ with $k\notin$ occ, $P_{k\mu}\geq 0.1$ have been included. The DIP's obtained from these calculations were substracted from $\text{IP}_c=696.43$ eV. Those lines with TR's greater than $P_c\times 10^{-5}$ a.u. $=0.748\times 10^{-5}$ a.u. are listed in Table II (the pole strengths of the DIP's are given in parentheses after the E_{kin} values). The dominating components of the

TABLE III. Auger spectrum of F_2, calculated using theoretical inner-valence IP's (energies in eV, transition rates in 10^{-3} a.u.).

Symmetry	E_{kin}	TR	Dominating components
$^1\Delta_g$	654.80(−0.805)	0.039	$1\pi_g^2(0.712)$, $1\pi_u^2(0.288)$
$^1\Sigma_g^+$	654.67(−0.804)	0.009	$1\pi_g^2(0.691)$, $1\pi_u^2(0.308)$
$^3\Pi_g$	647.18(−0.710)	0.061	$3\sigma_g^1 1\pi_g^3(0.991)$
$^1\Pi_g$	646.21(−0.777)	0.302	$3\sigma_g^1 1\pi_g^3(0.979)$
$^3\Pi_u$	644.87(−0.793)	0.051	$1\pi_u^3 3\sigma_g^1(0.957)$
$^1\Pi_u$	644.10(−0.791)	0.228	$1\pi_u^3 3\sigma_g^1(0.933)$
$^1\Delta_u$	642.74(−0.794)	0.361	$1\pi_u^3 1\pi_g^3(1.000)$
$^1\Delta_g$	642.17(−0.783)	0.334	$1\pi_u^2(0.681)$, $1\pi_g^2(0.319)$
$^1\Sigma_u^+$	641.46(−0.791)	0.086	$1\pi_u^3 1\pi_g^3(0.983)$
$^1\Sigma_g^+$	641.45(−0.806)	0.100	$1\pi_u^2(0.418)$, $3\sigma_g^0(0.369)$, $1\pi_g^2(0.208)$
$^1\Sigma_g^+$	640.20(−0.772)	0.124	$3\sigma_g^0(0.656)$, $1\pi_u^2(0.205)$, $1\pi_g^2(0.109)$
$^3\Pi_u$	635.32(−0.700)	0.021	$2\sigma_u^1 1\pi_g^3(0.833)$, $2\sigma_g^1 1\pi_u^3(0.111)$
$^1\Pi_g$	634.43(−0.563)	0.020	$2\sigma_g^1 1\pi_g^3(0.489)$, $2\sigma_u^1 1\pi_u^3(0.475)$
$^1\Pi_u$	633.59(−0.672)	0.060	$2\sigma_u^1 1\pi_g^3(0.661)$, $2\sigma_g^1 1\pi_u^3(0.254)$
$^3\Sigma_u^+$	630.16(−0.726)	0.025	$2\sigma_u^1 3\sigma_g^1(0.982)$
$^3\Pi_g$	630.05(−0.458)	0.031	$2\sigma_u^1 1\pi_u^3(0.824)$, $2\sigma_g^1 1\pi_g^3(0.166)$
$^3\Pi_u$	628.59(−0.359)	0.024	$2\sigma_g^1 1\pi_u^3(0.746)$, $2\sigma_u^1 1\pi_g^3(0.254)$
$^1\Pi_g$	627.43(−0.302)	0.059	$2\sigma_u^1 1\pi_u^3(0.963)$
$^1\Sigma_g^+$	626.09(−0.286)	0.039	$2\sigma_g^1 3\sigma_g^1(0.933)$
$^1\Pi_u$	625.82(−0.233)	0.071	$2\sigma_u^1 1\pi_g^3(0.689)$, $2\sigma_g^1 1\pi_u^3(0.292)$
$^1\Sigma_u^+$	624.78(−0.713)	0.155	$2\sigma_u^1 3\sigma_g^1(0.989)$
$^3\Pi_g$	620.54(−0.435)	0.024	$2\sigma_g^1 1\pi_g^3(0.932)$
$^3\Pi_u$	617.82(−0.382)	0.017	$2\sigma_g^1 1\pi_u^3(0.959)$
$^1\Sigma_g^+$	616.97(−0.475)	0.017	$2\sigma_u^0(0.593)$, $2\sigma_g^1 3\sigma_g^1(0.297)$
$^1\Pi_g$	616.33(−0.609)	0.164	$2\sigma_g^1 1\pi_g^3(0.759)$, $2\sigma_u^1 1\pi_u^3(0.238)$
$^1\Pi_u$	614.28(−0.550)	0.125	$2\sigma_g^1 1\pi_u^3(0.855)$, $2\sigma_u^1 1\pi_g^3(0.144)$
$^1\Sigma_u^+$	612.13(−0.044)	0.010	$2\sigma_g^1 2\sigma_u^1(0.928)$
$^1\Sigma_g^+$	611.24(−0.583)	0.106	$2\sigma_g^1 3\sigma_g^1(0.572)$, $2\sigma_u^0(0.364)$
$^1\Sigma_u^+$	609.16(−0.147)	0.033	$2\sigma_g^1 2\sigma_u^1(0.947)$
$^1\Sigma_g^+$	607.47(−0.223)	0.043	$2\sigma_g^0(0.521)$, $2\sigma_u^0(0.430)$
$^1\Sigma_u^+$	597.63(−0.481)	0.102	$2\sigma_g^1 2\sigma_u^1(0.977)$
$^1\Sigma_g^+$	593.23(−0.421)	0.045	$2\sigma_g^0(0.937)$

eigenvectors whose eigenvalues have the zero at $-\mathrm{DIP}_\nu$ are also indicated (the weights in parentheses are the squares of those components).

The more accurate proceeding would be, however, to use the theoretical data of Ref. 5 for the inner-valence IP's in the particle-particle Green's-function calculation. This has also been done, the other poles used being the same as those described above, and the results are listed in Table III. The two theoretical Auger spectra of Tables II and III are drawn as bar spectra in the figure (some pairs of quasidegenerate lines have been drawn as single lines) together with the experimental spectrum from Ref. 2.

The upper bar spectrum in Fig. 1 (cf. Table II) resembles qualitatively that obtained by WTJ (Ref. 2) by the Thomas-Weightman method,[15] in that the intermediate energy part is made up mainly of one strong group between ~ 620 and ~ 625 eV, while the experimental spectrum merely shows a gap at about this position. WTJ explained this failure with the neglect of the singlet-triplet splitting in their calculation and presumed that taking this splitting into account would shift the more intense singlet components into the region of intense spectral lines between ~ 616 and ~ 621 eV and the less intense triplet components into the weaker spectral features above ~ 626 eV. In our calculations, there was no neglect of singlet-triplet splittings and indeed the triplet lines range in the region above ~ 626 eV but have not enough intensity to explain by themselves the structures in that region. In fact, in our case the strong group between ~ 620 and ~ 625 eV is represented mainly by the singlets $^1\Pi_u$ (620.70 eV), $^1\Pi_g$ (621.60 eV), $^1\Sigma_g^+$ (622.37 eV), and $^1\Sigma_u^+$ (624.84 eV).

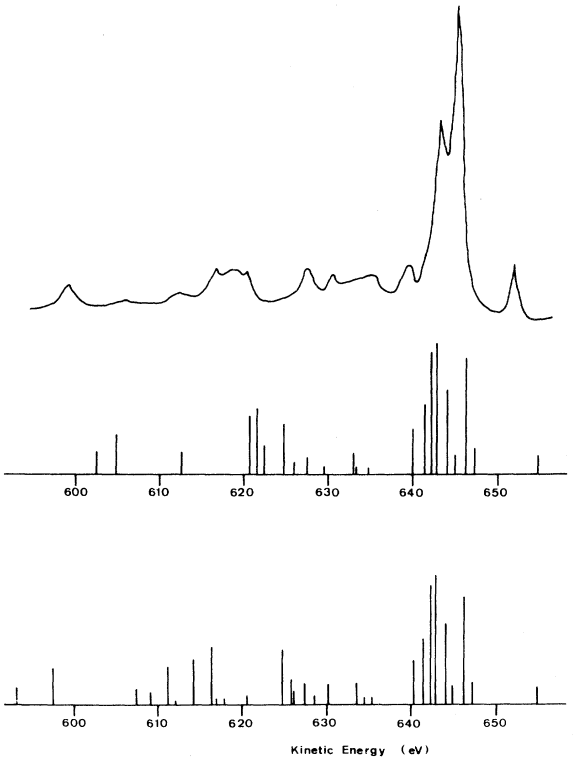

FIG. 1. Auger spectrum of F_2. Intensities are in arbitary units. Experimental spectrum of Ref. 2 has been shifted up from the abscissa. Upper bar spectrum is compiled from Table II, the lower from Table III.

Instead, our calculations predict the partial breakdown of the quasiparticle picture for the inner-valence electrons to be responsible for the splitting of this group. Proceeding to the lower bar spectrum in Fig. 1 (cf. Table III) we observe that some of the intensity of this group flows into a low-energy group composed mainly of $^1\Sigma_g^+$ (611.24 eV), $^1\Pi_u$ (614.28 eV), and $^1\Pi_g$ (616.33 eV), and some intensity into a high-energy group containing $^1\Sigma_u^+$ (624.78 eV), $^1\Sigma_g^+$ (626.09 eV), and $^1\Pi_g$ (634.43 eV). Indeed, the experimental (616—621)-eV group seems to be actually composed of three dominating peaks which would correspond to our $^1\Sigma_g^+$ (611.24 eV), $^1\Pi_u$ (614.24 eV), and $^1\Pi_g$ (616.33 eV). The high-energy group falls together with most of the corresponding triplets and also includes $^1\Pi_u$ (625.82 eV), $^1\Pi_g$ (627.43 eV), and $^1\Pi_u$ (633.59 eV). The leading experimental peak of this group at ~ 627 eV would then probably correspond to our $^1\Sigma_u^+$ (624.78 eV) while the following structures seem to represent a superposition of the numerous weaker lines in this region.

Let us also briefly consider the rest of the complete Auger spectrum. The pure outer-valence part above ~ 640 eV remains almost unaffected by the changes in the inner-valence IP's and there is little to be added to the findings of WTJ. In agreement with WTJ we associate the isolated high-energy peak at ~ 652 eV with $^1\Sigma_g^+$ (654.67 eV) and $^1\Delta_g$ (654.80 eV). In their calculation within the Thomas-Weightman[15] model WTJ obtained all other pure outer-valence lines in the (639—647)-eV interval while in their final assignments they used the independent-particle result for $^1\Sigma_g^+$ ($3\sigma_g^0$) and associated it with the experimental 635-eV feature. Our calculations would favor the former of these possibilities, and we interpret the 637-eV gap as the visible boundary of the pure outer-valence part of the Auger spectrum. The lines within the (639—647)-eV group are so closely spaced that we do not attempt a more detailed analysis of this group on the basis of the present results.

One might expect the lowest-energy part of the spectrum to be most sensitive to the mode of description of the inner-valence electrons. Surprisingly, however, the improvements in this region after inclusion of the breakdown effects are less obvious. Instead, the narrowness of the main peak, which is unusual in this part of the spectrum,[2] seems to argue against spectacular breakdown effects.

The situation can be understood as follows: Unlike many other molecules F_2 has only a partial breakdown of the quasiparticle picture for its inner-valence electrons, the quasiparticle lines are split into only very few lines (instead of into numerous lines as in the more frequent case of a complete breakdown of the quasiparticle picture for inner-valence electrons[3]). This is why the corresponding approximate IP's could still be extracted from the photoelectron spectrum, and this is also the reason for the narrowness of the individual lines in the Auger spectrum.

In the upper bar spectrum $^1\Sigma_g^+$ (602.57 eV) and $^1\Sigma_u^+$ (604.93 eV) seem to be responsible for the experimental 599-eV peak; this also corresponds to the assignment of WTJ. Proceeding to the lower bar spectrum these two lines are split into the pair $^1\Sigma_g^+$ (593.23 eV) and $^1\Sigma_u^+$ (597.63 eV) and, well separated, the pair $^1\Sigma_g^+$ (607.47 eV)

and $^1\Sigma_u^+$ (609.16 eV). We associate the pair $^1\Sigma_g^+$ (607.47 eV) and $^1\Sigma_u^+$(609.16 eV) with the 612-eV feature and have thus reproduced the wide, essentially structure-free, interval seen in the experimental spectrum between the 599-eV peak and the 612-eV feature.

It is noteworthy that the intensity splitting is rather different for $^1\Sigma_g^+$ and $^1\Sigma_u^+$. While the two $^1\Sigma_g^+$ lines have almost equal intensity, there is a strong asymmetry for the $^1\Sigma_u^+$ intensity splitting which makes $^1\Sigma_u^+$ (597.47 eV) the dominating line. It would be tempting to assign the 599-eV peak only to this dominating line, because the observed peak is so narrow. Furthermore, the spacing between $^1\Sigma_g^+$ (593.23 eV) and $^1\Sigma_u^+$ (597.63 eV) is even larger than the corresponding spacing in the upper bar spectrum which argues against a quasidegeneracy of these levels. It would then have to be assumed that the $^1\Sigma_g^+$ (593.23 eV) line is hidden by the background. This question of assignment will not be settled here, the more so since the experimental spectrum ends at about 595 eV.

IV. CONCLUSION

We have given reasons to believe that the pronounced gap seen in the experimental Auger spectrum of F_2 at 621–626 eV is a consequence of the satellite structure of the inner-valence IP's, corresponding to a partial breakdown of the quasiparticle picture for those electrons. Since this satellite structure is not resolved in the experimental photoelectron spectrum, we have found an example where Auger electron spectroscopy can be used to probe details of the photoelectron spectrum which would otherwise be beyond the limits of experimental confirmation.

ACKNOWLEDGMENTS

My thanks to Dr. D. R. Jennison for communicating Ref. 2 prior to publication, and to the Wissenschaftliches Rechenzentrum Berlin (WRZ) and Zentraleinrichtung Rechenzentrum (ZRZ) of the Technische Universitat Berlin for computer time.

[1]For recent reviews see H. Ågren, J. Chem. Phys. 75, 1267 (1981); D. R. Jennison, J. Vac. Sci. Technol. 20, 548 (1982), and references therein.

[2]P. Weightman, T. D. Thomas, and D. R. Jennison, J. Chem. Phys., 78, 1652 (1983).

[3]L. S. Cederbaum, J. Schirmer, W. Domcke, and W. von Niessen, J. Phys. B 10, L549 (1977); Int. J. Quantum Chem. 14, 593 (1978).

[4]C.-M. Liegener, Chem. Phys. Lett. 90, 188 (1982).

[5]W. von Niessen, G. H. F. Diercksen, and L. S. Cederbaum, J. Chem. Phys. 67, 4124 (1977); G. Bieri, L. Åsbrink, and W. von Niessen, J. Electron Spectrosc. 23, 281 (1981).

[6]L. S. Cederbaum, G. Hohlneicher, and S. Peyerimhoff, Chem. Phys. Lett. 11, 421 (1971); L. S. Cederbaum, Theoret. Chim. Acta 31, 239 (1973); L. S. Cederbaum, G. Hohlneicher, and W. von Niessen, Mol. Phys. 26, 1405 (1973).

[7]H. Siegbahn, L. Asplund, and P. Kelfve, Chem. Phys. Lett. 35, 330 (1975).

[8]D. R. Jennison, Chem. Phys. Lett. 69, 435 (1980); Phys. Rev. A 23, 1215 (1981).

[9]E. U. Condon and G. H. Shortley, *The Theory of Atomic Spectra* (Cambridge University, Cambridge, England, 1935).

[10]E. J. McGuire, Phys. Rev. 185, 1 (1969).

[11]T. H. Dunning, Jr., J. Chem. Phys. 53, 2823 (1970).

[12]K. P. Huber and G. Herzberg, *Constants of Diatomic Molecules* (Van Nostrand, Princeton, 1979).

[13]L. S. Cederbaum and W. Domcke, Adv. Chem. Phys. 36, 205 (1977).

[14]G. Bieri, A. Schmelzer, L. Åsbrink, and M. Jonsson, Chem. Phys. 49, 213 (1980).

[15]T. D. Thomas and P. Weightman, Chem. Phys. Lett. 81, 325 (1981).